On Hyperbolic Attractors in a Modified Complex Shimizu – Morioka System

V.P. Kruglov[1] and I.R. Sataev[1]
Kotelnikov's Institute of Radio-Engineering and Electronics of RAS, Saratov Branch, Zelenaya 38, Saratov, 410019, Russia

(*Electronic mail: sataevir@gmail.com)

(*Electronic mail: kruglovyacheslav@gmail.com)

(Dated: 24 April 2023)

We present a modified complex-valued Shimizu – Morioka system with a uniformly hyperbolic attractor. We show that the numerically observed attractor in the Poincaré cross-section expands 3 times in the angular direction and strongly contracts in the transversal directions, similar in structure to the Smale – Williams solenoid. This is the first example of a modification of a system with a genuine Lorenz attractor, but manifesting a uniformly hyperbolic attractor instead. We perform numerical tests to show the transversality of tangent subspaces, a pivotal property of uniformly hyperbolic attractors, for both the flow system and its Poincaré map. We also observe that no genuine Lorenz-like attractors appear in the modified system.

Historically, after seminal works[1,2] by Afraimovich, Bykov and Shilnikov, homoclinic "butterfly" bifurcation is often associated with the scenario of the birth of the Lorenz attractor. The Lorenz attractor is a robustly chaotic system that appears in various physical problems, from models of atmospheric instability to lasers and mechanical systems. In this article, we demonstrate for the first time that the homoclinic "butterfly" bifurcation can also give rise to uniformly hyperbolic chaotic attractors, which are a different type of robust chaos. We introduced earlier[3] a class of autonomous flow models with complex variables that can demonstrate attractors of the Smale – Williams type. These models result from a specific complexification of real-valued two-dimensional systems that demonstrate homoclinic bifurcation of the separatrix loop. Now for the first time we use the bifurcation of a homoclinic "butterfly" as a basic homoclinic bifurcation – a construction only possible in three dimensions. Unlike two-dimensional case such bifurcation may lead to chaotic attractors of Lorenz or Rovella[4–6] type depending on the sign of the saddle value. One of the simplest models with homoclinic "butterfly" bifurcation is the three-dimensional Shimizu – Morioka system. We consider a modification of the complex-valued version of this system that demonstrates a uniformly hyperbolic chaotic attractor of the Smale – Williams type. S.P. Kuznetsov was the first to suggest a physical system with a Smale – Williams attractor[7]. Later, Kuznetsov and others proposed a number of systems with Smale – Williams type attractors, including physically realizable ones[8–11]. However, these systems were specially synthesized to obtain such an attractor and turned out to be extremely artificial and complicated. The complex Shimizu-Morioka system offers a unique opportunity since it arises in physical applications and is in a form suitable for obtaining a modification with a hyperbolic attractor.

I. INTRODUCTION

Complex-valued Lorenz and Shimizu – Morioka systems have been previously studied in detail[12,13]. The Shimizu – Morioka system is a transformed and simplified version of the Lorenz system. These systems are found in physical problems such as detuned lasers[14] and baroclinic instability in two-layered rotating fluids[15–17]. Fowler and Gibbon stated[18] that complex and real-valued Lorenz models arise naturally in dispersive unstable systems with weak dissipation, in contrast to the truncated real-valued model of two-dimensional convection with high dissipation studied by Lorenz[19].

The complex Shimizu-Morioka system[12,13] is given by eq. (1):

$$\begin{aligned}\dot{x} &= y,\\ \dot{y} &= -\mu y + (1-z)x,\\ \dot{z} &= -\alpha z + |x|^2.\end{aligned} \tag{1}$$

where x and y are complex variables, and z is real. Parameters μ and α are also real. The equation for z only depends on the absolute value of x, since z is a real variable. The equations are symmetric under transformation $(x, y, z) \to \left(xe^{i\phi}, ye^{i\phi}, z\right)$ and therefore invariant under phase shifts.

The real-valued Shimizu – Morioka system is written as follows, where X and Y are real:

$$\begin{aligned}\dot{X} &= Y,\\ \dot{Y} &= -\mu Y + (1-Z)X,\\ \dot{Z} &= -\alpha Z + X^2.\end{aligned} \tag{2}$$

It demonstrates homoclinic "butterfly" bifurcation[20] with both positive and negative saddle values[21,22]. We present here a number of numerical evidences that the complex Shimizu – Morioka system (1) under a small perturbation can manifest a uniformly hyperbolic chaotic attractor in a vicinity of the point with parameter values corresponding to the "butterfly" bifurcation with the negative saddle value.

Uniformly hyperbolic chaotic attractors are the most refined geometric shapes of chaos[11,23–28]. They have been rigorously proven to be genuine chaotic attractors. All trajectories belonging to uniformly hyperbolic attractors are of saddle type, with the same dimensions of stable, neutral, and unstable subspaces. What is most important is that the tangent subspaces are transversal to each other at every point on the uniformly hyperbolic attractor and in its vicinity. These fine geometrical features ensure that the attractor is structurally stable, meaning it preserves its structure under small perturbations of the governing equations.

It is worth mentioning that there is another wider class of genuine chaotic attractors called pseudohyperbolic[29,30]. While they are not structurally stable, they still preserve their most important features under perturbations. The definition of pseudohyperbolicity is less strict than that of uniformly hyperbolic attractors, with the latter being a special subclass of the former.

The Lorenz attractor is pseudohyperbolic[31]. Unlike uniformly hyperbolic attractors, the Lorenz attractor is singular, containing the saddle equilibrium with its unstable separatrices. There is a dense set of parameter values at which the separatrices become bi-asymptotic to the saddle. As a result, the Lorenz attractor is not structurally stable, even though it remains chaotic under changes of parameters. The Lorenz system attractor has a continuous invariant of topological equivalence known as the kneading invariant. Thus, the structure of the attractor changes continuously when this invariant changes[32,33].

There are also wild pseudohyperbolic attractors[29,34]. Unlike uniformly hyperbolic attractors, they allow tangencies between subspaces but do not generate stable orbits under perturbations. Pseudohyperbolic attractors are robustly chaotic. In comparison, the most common type of attractors in applications, called quasi-attractors[35], are not robustly chaotic. This is because they manifest zero angles between subspaces and birth of stable orbits at small perturbations.

The Smale – Williams solenoid is one of the conceptual geometrical examples of uniformly hyperbolic attractors[24,36]. It appears in an absorbing toroidal domain of the phase space of dimension 3 (or more) under the action of a diffeomorphism expanding the domain integer times (2, 3, etc.) in the longitudinal (angular) direction, contracting it in all transverse directions, and folding inside. The result of the infinite iterations is a uniformly hyperbolic attractor having a local structure of the product of a Cantor set and an interval. What is really important here is that the diffeomorphism in the restriction to the angular variable (factor-map) has the form of a Bernoulli map. Figure 1 shows the toroidal domain and its image under the action of the map with an expansion factor of 3 (panel a), the resulting attractor at $n \to \infty$ (panel b), the transversal Cantor set structure of its filaments (panel c), and the θ_{n+1} vs. θ_n diagram for the kind of Bernoulli map $\theta_{n+1} = 3\theta_n + \pi \pmod{2\pi}$.

Attractors similar to the Smale – Williams solenoid appear in Poincaré cross-sections of specially designed mathematical and physical models (electronic or mechanical) by Kuznetsov[7,8,10,11], in which the phase of the oscillations is

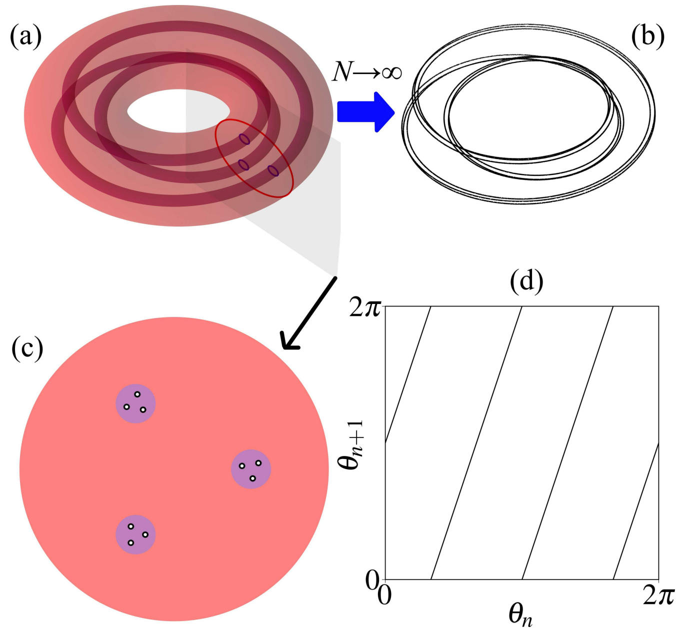

FIG. 1. (a) The action of the map stretches the toroidal domain 3 times in a direction around the hole but strongly contracts in other directions and folds inside the initial domain; (b) The solenoid with an expansion factor of three appears in the limit as $n \to \infty$. (c) The images of the absorbing domain are shown in a transversal cut, and in the limit, the Cantor set appears. (d) The θ_n vs. θ_{n+1} diagram for the Bernoulli map $\theta_{n+1} = 3\theta_n + \pi \pmod{2\pi}$ corresponds to the previous pictures. A π shift is also observed in our complex Shimizu – Morioka model. The exact equations to produce these pictures can be found in our previous article on the topic[3].

usually the angular variable under the Bernoulli map. The hyperbolicity of the attractor of the model from[7] has been confirmed by computer-assisted proofs[37,38].

Recently, we studied a peculiar system of differential equations with complex variables in which the emergence of a hyperbolic attractor of Smale – Williams type is observed in numerics and is geometrically interpretable and explainable[3]. The model is derived from a self-oscillatory real-valued system with a homoclinic bifurcation of the saddle equilibrium: at some parameter value, stable limit cycles glue into the separatrix loops forming a homoclinic figure eight[39,40]. In the complexified system, there is a saddle equilibrium at the origin with two equal positive eigenvalues and two equal negative eigenvalues. There is also a special perturbation providing integer times expansion of the arguments of complex variables (on 2π average) when the trajectory passes near the saddle. In a vicinity of the saddle, the trajectory turns to an angle governed by a map close to the Bernoulli map. The presence of a homoclinic loop ensures the return of the trajectory to the saddle. We have checked numerically that the stable and unstable tangent subspaces of the attractor in the Poincaré cross-section are always transversal. We have also observed the structural stability and other properties of a uniformly hyperbolic attractor. Therefore, we have concluded that the system indeed possesses a hyperbolic attractor of Smale – Williams type.

The complex Shimizu – Morioka system may also be considered as a complexification of the real-valued system

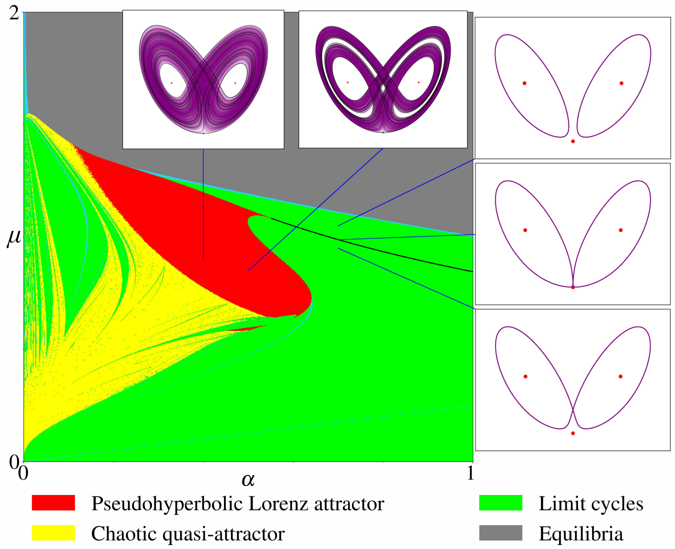

FIG. 2. The chart of regimes of the Shimizu – Morioka model (2), μ vs. α, is obtained numerically by calculating the Lyapunov exponents and checking the transversality of tangent subspaces. In the yellow regions, chaotic quasi-attractors appear. In the red region, pseudohyperbolic Lorenz attractors manifest. In the green regions, there is no chaos, but stable limit cycles appear. The black line outlines the homoclinic bifurcation with the negative saddle value. In the grey region, the only attractors are equilibria. The two upper panels contain examples of pseudohyperbolic Lorenz attractors: at $\mu = 0.9$, $\alpha = 0.4$ and at $\mu = 0.85$, $\alpha = 0.5$. The three side panels demonstrate the stable homoclinic butterfly at $\mu \approx 0.98695\ldots$, $\alpha = 0.7$ (the saddle at the origin has a negative saddle value) and two phase space configurations near it. See articles[21,22,43,44] to compare the charts.

demonstrating the homoclinic loop. It appears to be suitable for perturbation leading to the birth of the hyperbolic attractor.

In Section II, we discuss the classical Shimizu – Morioka system and construct its complex modification. In Section III, we provide the results of numerical studies of the complex Shimizu – Morioka system, including portraits of attractors and Lyapunov exponents. In Section IV, we discuss the criteria of angles – the technique used to determine if the attractor is uniformly hyperbolic, pseudohyperbolic, or a quasi-attractor. We also present the results of the test applied to our model and provide charts of regimes.

II. THE COMPOSITION OF COMPLEX-VALUED SHIMIZU – MORIOKA EQUATIONS

The Shimizu – Morioka system (2) has been extensively investigated, see[21,41,42] for example. The system (2) is invariant under the transformation $(x, y, z) \to (-x, -y, z)$ and has three equilibria for $\mu > 0$, $\alpha > 0$: the saddle $O = (0, 0, 0)$ and two foci or saddle-foci $O_{1,2} = \left(\pm\sqrt{\alpha}, 0, 1\right)$.

The Shimizu – Morioka system (2) has been proved to manifest a genuine Lorenz attractor, as demonstrated in[42]. The formation of the Lorenz attractor is a result of the homoclinic bifurcation of the saddle equilibrium with a positive saddle value $\sigma = \lambda_1 + \lambda_2$, where λ_1 is the positive eigenvalue of the saddle and λ_2 is the closest to zero negative eigenvalue. However, this paper focuses on a homoclinic bifurcation with the negative saddle value, which results in the gluing of stable limit cycles into bi-asymptotic separatrices of the saddle. In the classical three-dimensional Shimizu-Morioka system (2), such a bifurcation does not lead to the formation of a chaotic attractor.

Fig. 2 displays the chart of regimes for system (2). The thick black curve outlines the loci of the stable homoclinic "butterfly" (homoclinic "butterfly" bifurcation with the negative saddle value). The panels inserted on the side demonstrate the homoclinic "butterfly" at $\alpha = 0.7$, $\mu \approx 0.98695\ldots$, and the phase space configurations forming near these parameter values. We evaluated the bifurcation line numerically using a crude algorithm: the parameter space was scanned for situations where limit cycles start to visit both positive and negative parts of the phase space relative to the plane $x = 0$. Other regimes were checked by calculating the Lyapunov exponents with standard methods[45–47]. If the largest Lyapunov exponent is negative, the attractor is a simple equilibrium, one of two foci $O_{1,2}$ (marked grey on the chart). If the largest Lyapunov exponent is zero up to numerical accuracy, the attractor is a limit cycle (marked green). If the largest Lyapunov exponent is positive, the attractor is chaotic. We performed a special test for pseudohyperbolicity, developed in[48,49], which we discuss in detail in Section IV. Pseudohyperbolic Lorenz attractors are marked red, and chaotic quasi-attractors are marked yellow on the chart. Similar charts can be found in[21,22,43,44]. The region of genuine Lorenz attractors is continuous because the existence of a Lorenz attractor is a robust property[2]. However, in this paper, we are interested in constructing a uniformly hyperbolic attractor, and the test for pseudohyperbolicity is only carried out simultaneously with the test for uniform hyperbolicity.

The linearized at the origin complex Shimizu – Morioka system (1) is given by:

$$\begin{aligned} \dot{x} &= y, \\ \dot{y} &= -\mu y + x, \\ \dot{z} &= -\alpha z. \end{aligned} \tag{3}$$

The first two equations are the same as those considered in[3] and are suitable for perturbation, leading to an integer times expansion of the arguments of complex variables (on a 2π average) when the trajectory passes close to the saddle. Taking into account the returns of the trajectories to the vicinity of the origin due to nonlinear terms, we suggest that the perturbed version of the complex Shimizu – Morioka system demonstrates a Bernoulli-like map for the arguments of complex variables.

We added the perturbation εy^3 to the system (1), similar to what was done in[3]:

$$\begin{aligned} \dot{x} &= y, \\ \dot{y} &= -\mu y + (1 - z)x + \varepsilon y^3, \\ \dot{z} &= -\alpha z + |x|^2. \end{aligned} \tag{4}$$

Perturbations such as εy^2 and εy^4 are also possible, but they do not preserve the symmetry $(x, y, z) \to (-x, -y, z)$, unlike

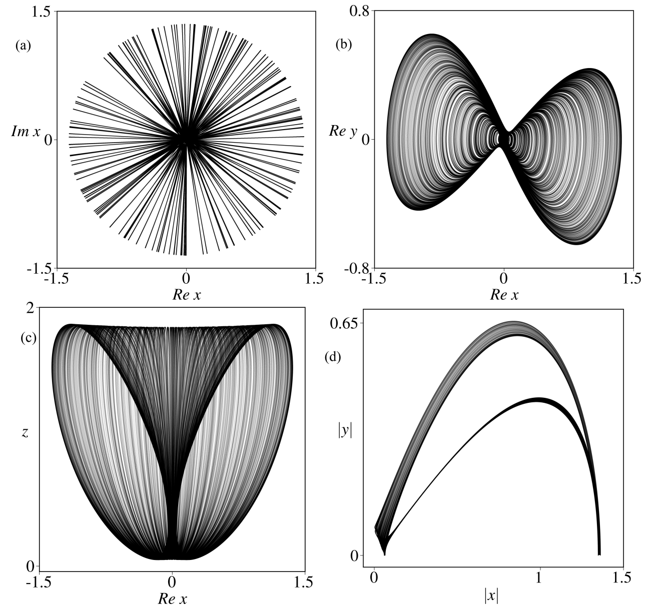

FIG. 3. Projections of the attractor and the dynamics of absolute values for the flow system (4) with parameter values $\mu = 0.98$, $\alpha = 0.7$, and $\varepsilon = 0.1$. Panel (a) shows the projection of the uniformly hyperbolic attractor onto the plane of variables $(\mathrm{Re}\,x, \mathrm{Im}\,x)$. Panel (b) shows the projection onto the $(\mathrm{Re}\,x, \mathrm{Re}\,y)$ plane. Panel (c) shows the projection onto the $(\mathrm{Re}\,x, z)$ plane. Panel (d) shows the dynamics of the absolute values $|x|$ and $|y|$.

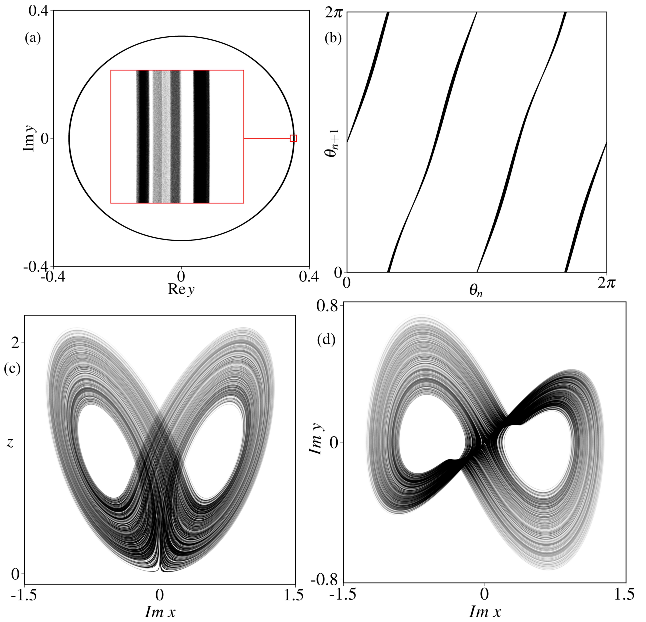

FIG. 4. Panel (a) shows the portrait of the attractor of the Poincaré map and an enlarged part of it. Panel (b) shows the diagram of θ_{n+1} vs. θ_n. The parameter values for both panels (a) and (b) are $\mu = 0.98$, $\alpha = 0.7$, and $\varepsilon = 0.1$. Panel (c) shows the projection of the non-hyperbolic attractor of the flow system (4) onto the $(\mathrm{Im}\,x, z)$ plane, and panel (d) shows the projection onto the $(\mathrm{Im}\,x, \mathrm{Im}\,y)$ plane. The parameter values for panels (c) and (d) are $\mu = 0.9$, $\alpha = 0.4$, and $\varepsilon = 0.1$.

εy^3. We preserve this symmetry to achieve a more homogeneous distribution of the natural measure on the attractor. The system (4) has five real variables overall: $\mathrm{Re}\,x$, $\mathrm{Im}\,x$, $\mathrm{Re}\,y$, $\mathrm{Im}\,y$ and z. The saddle at the origin has two pairs of equal eigenvalues: $\lambda_{1,2} = -\frac{\mu}{2} + \frac{\sqrt{\mu^2+4}}{2} > 0$ and $\lambda_{3,4} = -\frac{\mu}{2} - \frac{\sqrt{\mu^2+4}}{2} < 0$; there is also an eigenvalue $\lambda_5 = -\alpha < 0$.

Suppose the parameters are close to the values for the stable homoclinic butterfly in the original system. While the original system (2) supports only stable limit cycles at such parameters, our modified complex system (4) exhibits instability along the argument of the complex variable x. The only term in (4) that changes the arguments of variables is the perturbation εy^3. One can notice that both complex variables x and y have arguments, but the arguments are actually constrained to each other. They change simultaneously due to $y = \dot{x}$ with a constant π shift. They correspond to the same expanding angular variable, and this statement is verified in numerical simulations (there is only one positive Lyapunov exponent, for example).

The typical trajectory of (4) returns to the vicinity of the saddle at the origin along the stable invariant manifold. This causes the angle in the complex plane $(\mathrm{Re}\,x, \mathrm{Im}\,x)$ to undergo multiplication based on the degree of perturbation introduced. We call this phenomenon the "scattering" of trajectories on the saddle, as described in detail in[3]. The equations (4) almost preserve the symmetry $(x, y, z) \to \left(xe^{i\phi}, ye^{i\phi}, z\right)$ for small values of ε, which means that the angle remains unchanged in the complex plane $(\mathrm{Re}\,x, \mathrm{Im}\,x)$ when the state is far from the origin. Therefore, with each pass near the origin, the angle changes in accordance with the Bernoulli map.

III. RESULTS OF NUMERICAL SIMULATIONS OF THE COMPLEX-VALUED SHIMIZU – MORIOKA EQUATIONS

The numerical solutions of Equations (4) were obtained using the Runge-Kutta 4$^{\text{th}}$ order method. Fig. 3 displays the attractor of the flow system at $\lambda = 0.98$, $\alpha = 0.7$, and $\varepsilon = 0.1$ in various projections. Fig. 3(a) shows the projection of the attractor onto the plane $(\mathrm{Re}\,x, \mathrm{Im}\,x)$. The trajectory runs along straight lines far from the saddle and turns to different directions only near the saddle. Fig. 3(b) displays the projection onto the $(\mathrm{Re}\,x, \mathrm{Re}\,y)$ plane, where the portrait of the attractor visually resembles a filled figure eight. Between successful scatterings on the saddle, the trajectory revolves around points of the circle of equilibria $\left(\sqrt{\alpha}e^{i\theta}, 0, 1\right)$, where $\theta \in [0, 2\pi)$. Each turn is at a different angle θ, resulting in the portrait of the attractor being filled with loops. Fig. 3(c) shows another projection onto the $(\mathrm{Re}\,x, z)$ plane, which is consistent with the explanation of panels (a) and (b). Although we consider the variable z unimportant for scattering, it is required for the return of the trajectory to the vicinity of the saddle. Fig. 3(d) displays the dynamics of the absolute values $|x|$ and $|y|$. The trajectory goes from and back to the saddle but is always at a finite distance from it (we have verified this numerically for very long simulation times). In contrast, trajectories of the pseudohyperbolic Lorenz attractor come arbitrarily close to the saddle.

We constructed an appropriate Poincaré cross-section surface of the flow (4): $S := z - 1 = 0$ (when trajectories go from $z < 1$ to $z > 1$). Fig. 4(a) displays the attractor of the Poincaré return map and its enlarged part for $\lambda = 0.98$, $\alpha = 0.7$, and $\varepsilon = 0.1$ (the same values as in Fig. 3). We consider it an attractor of Smale – Williams type, with features similar to the Smale – Williams solenoid in Fig. 1(b). The enlarged part demonstrates the transversal fractal structure of the attractor. Fig. 4(b) shows the diagram of θ_{n+1} vs. θ_n, which is clearly close to the Bernoulli map $\theta_{n+1} = 3\theta_n + \pi \pmod{2\pi}$. We have numerically verified that the map for the argument θ is continuous and monotonous, with a topological factor of expansion equal to 3. The procedure has been implemented previously[3]: we split the 2π interval into $N = 1000$ pieces, iterate the map 10^6 times, and accumulate the averages $\Phi_k = \frac{1}{T_k}\sum_{n=0}^{T_k} e^{i\theta_n}$ of θ_n values that land in the k-th interval, where $k \in [0, N-1]$ is the index of the small interval, and T_k is the count of $e^{i\theta_n}$ that land in the small interval k. We verify the absence of empty intervals after a sufficiently long time of numerical simulation: if the count T_k of every interval is nonzero, the transformation is continuous. If all angular shifts $\arg\Phi_{k+1} - \arg\Phi_k$ between neighboring intervals are positive, then the transformation is monotonous. Finally, we calculate the sum $M = \frac{1}{2\pi}\sum_{k=0}^{N-1}(\arg\Phi_{k+1} - \arg\Phi_k)$, which is the expanding factor of the transformation. The expanding factor M is exactly 3 in our calculations for parameter values $\mu = 0.98$, $\alpha = 0.7$, and $\varepsilon = 0.1$.

The Lyapunov exponents for the flow attractor with parameter values $\lambda = 0.98$, $\alpha = 0.7$, $\varepsilon = 0.1$ are:

$$\begin{aligned}
\lambda_1 &= 0.0959 \pm 0.0005,\\
\lambda_2 &= 0 \pm 0.0001,\\
\lambda_3 &= -0.126 \pm 0.003,\\
\lambda_4 &= -1.060 \pm 0.001,\\
\lambda_5 &= -1.571 \pm 0.003.
\end{aligned} \tag{5}$$

The first exponent is positive, as expected for a chaotic attractor, the second is zero, as expected for an autonomous system, and the others are negative. Note that every contraction is stronger than expansion: $\lambda_1 < |\lambda_3|$. The Lyapunov dimension of the flow attractor is given by the Kaplan – Yorke formula[50]: $D_{KY} = 2 + \frac{\lambda_1+\lambda_2}{|\lambda_3|} = 2.761$.

The average time interval between successful Poincaré cross sections is $T_{av} = 11.331$. The largest Lyapunov exponent for the Poincaré map is $\Lambda_1 = T_{av}\lambda_1 = 1.086$, which is approximately equal to $\ln 3$, the Lyapunov exponent for the Bernoulli map with an expansion factor of 3. Overall, the attractor of the Poincaré map exhibits the features of a Smale – Williams type attractor.

Different kinds of chaotic attractors are possible at different parameter values. For example, in the classical Shimizu – Morioka system (2) with $\lambda = 0.9$ and $\alpha = 0.4$, the Lorenz attractor emerges. A very similar attractor appears in the modified system (4) with $\lambda = 0.9$, $\alpha = 0.4$, and $\varepsilon = 0.1$, as shown in Fig. 4(c) and (d). Interestingly, the trajectories of this attractor do not oscillate in the directions of $\mathrm{Re}\,x$ and $\mathrm{Re}\,y$; only $\mathrm{Im}\,x$, $\mathrm{Im}\,y$, and z are non-zero, and the attractor is visually confined to three-dimensional space. Its Lyapunov exponents are:

$$\begin{aligned}
\lambda_1 &= 0.0348 \pm 0.0003,\\
\lambda_2 &= 0 \pm 0.0001,\\
\lambda_3 &= -0.014 \pm 0.001,\\
\lambda_4 &= -0.905 \pm 0.001,\\
\lambda_5 &= -1.3548 \pm 0.0002.
\end{aligned} \tag{6}$$

Note that there are contractions weaker than expansion: $\lambda_1 > |\lambda_3|$. The Lyapunov dimension of the flow attractor, as given by the Kaplan – Yorke formula, is $D_{KY} = 3 + \frac{\lambda_1+\lambda_2+\lambda_3}{|\lambda_4|} = 3.023$. This is larger than the Lyapunov dimension of the uniformly hyperbolic attractor, and even slightly larger than 3, despite the fact that the attractor appears to be embedded in 3D space. It also differs from the Kaplan – Yorke dimension of the classical Lorenz attractor (2) with $\lambda = 0.9$ and $\alpha = 0.4$, which is $D_{KY} = 2.031$. Although the attractor looks very similar to the Lorenz attractor, it is quantitatively different.

IV. NUMERICAL TEST OF HYPERBOLICITY

The pivotal feature of uniformly hyperbolic attractors is the transversality of the stable E^s, neutral E^n, and unstable E^u subspaces of the tangent space at every point of the attractor[51,52]. To compute this, we use a fast numerical algorithm[48] based on the covariant Lyapunov vectors computation procedures[53].

For an autonomous flow governed by $\dot{\mathbf{x}} = \mathbf{f}(\mathbf{x})$ in an m-dimensional phase space, we solve numerically $k \le m-1$ variational equations

$$\dot{\mathbf{u}} = \hat{\mathbf{J}}(\mathbf{x}) \cdot \mathbf{u}, \tag{7}$$

where $\hat{\mathbf{J}}(\mathbf{x})$ is the Jacobi matrix of $\mathbf{f}(\mathbf{x})$, along a typical trajectory on the attractor. We orthogonalize and normalize the perturbation vectors regularly using the Gram – Schmidt procedure. This gives us fields of k perturbation vectors $\mathbf{u}(t)$ along the trajectory, which we store in computer memory.

We also solve k adjoint variational equations

$$\dot{\mathbf{v}} = -\hat{\mathbf{J}}^{\mathsf{T}}(\mathbf{x}) \cdot \mathbf{v} \tag{8}$$

along the same trajectory backwards in time, where $\hat{\mathbf{J}}^{\mathsf{T}}(\mathbf{x})$ is the transposed Jacobi matrix. To prevent divergence due to instability of backward time calculation, we store the trajectory in computer memory while solving in forward time. We obtain and store fields of k vectors $\mathbf{v}(t)$, which are orthogonal to some subspace of dimension $m-k$. It is important to note that if we evaluate k Lyapunov exponents alongside solving for $\mathbf{u}(t)$ in forward time and for $\mathbf{v}(t)$ in backward time, then the Lyapunov exponents must coincide in pairs.

We compile fields of matrices $\hat{\mathbf{U}}(t)$ and $\hat{\mathbf{V}}(t)$ with k columns from vectors $\mathbf{u}(t)$, $\mathbf{v}(t)$ and m rows. Using these matrices, we compute $k \times k$ matrices $\hat{\mathbf{P}}(t) = \hat{\mathbf{V}}^{\mathsf{T}}(t) \cdot \hat{\mathbf{U}}(t)$, which contain information about the local structure of the attractor.

If the matrix $\hat{\mathbf{P}}$ is singular at some point $\mathbf{x}$, then the k-dimensional space spanned by the columns of $\hat{\mathbf{U}}$ and the $m-k$-dimensional space orthogonal to the columns of $\hat{\mathbf{V}}$ are tangent

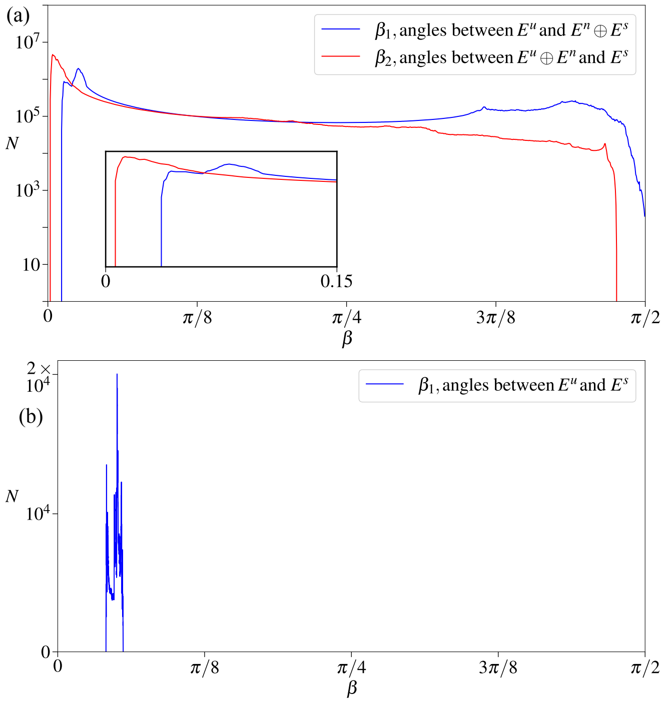

FIG. 5. (a) The distributions of angles between subspaces of the attractor of the flow system (4) at $\mu = 0.98$, $\alpha = 0.7$, $\varepsilon = 0.1$. (b) The distribution of angles between subspaces of the Poincaré map at $\mu = 0.98$, $\alpha = 0.7$, $\varepsilon = 0.1$.

at this point. A matrix is singular if its determinant is zero or, equivalently, if its minimal singular value σ_k is zero. The minimal singular values σ_k are related to the angles between subspaces $\beta_k = \frac{\pi}{2} - \arccos\sigma_k$.

The algorithm can also be applied to diffeomorphisms $\mathbf{x}_{n+1} = \mathbf{F}(\mathbf{x}_n)$. In this case, the variational equations are:

$$\mathbf{u}_{n+1} = \hat{\mathbf{J}}(\mathbf{x}_n) \cdot \mathbf{u}_n, \qquad (9)$$

where $\hat{\mathbf{J}}(\mathbf{x})$ is the Jacobi matrix of $\mathbf{F}(\mathbf{x})$. The adjoint variational equations in forward time are

$$\mathbf{v}_{n+1} = \hat{\mathbf{J}}^{-\mathsf{T}}(\mathbf{x}_n) \cdot \mathbf{v}_n, \qquad (10)$$

where $\hat{\mathbf{J}}^{-\mathsf{T}}(\mathbf{x})$ is the inversed and transposed Jacobi matrix. In backward time, equation (10) transforms to $\mathbf{v}_n = \hat{\mathbf{J}}^{\mathsf{T}}(\mathbf{x}_n) \cdot \mathbf{v}_{n+1}$.

In our experience, the matrices $\hat{\mathbf{P}}(t)$ converge faster for the Poincaré map than for the flow. However, the correct way to compute the angles between subspaces is for the attractor of the flow. This is because the naive choice of a Poincaré cross-section can lead to incorrect conclusions. Some parts of the phase space might have prominent tangencies between subspaces, while others might have very rare and hard-to-find tangencies.

The trajectories of the attractor of the flow (4) at $\mu = 0.98$, $\alpha = 0.7$, $\varepsilon = 0.1$ have a 1-dimensional unstable subspace E^u, a 1-dimensional neutral subspace E^n, and a 3-dimensional stable subspace E^s, according to Lyapunov exponents (5). Therefore, it is sufficient to compute two perturbation vectors in forward and backward time and obtain 2×2 matrices $\hat{\mathbf{P}}(t)$.

The upper left elements of $\hat{\mathbf{P}}(t)$ are scalar products of perturbation vectors $\mathbf{u}_1(t)$, spanning the unstable subspace E^u, and vectors $\mathbf{v}_1(t)$ orthogonal to the sum of subspaces $E^n \oplus E^s$: $\sigma_1 = \mathbf{u}_1(t) \cdot \mathbf{v}_1(t)$. Therefore, the corresponding angles $\beta_1 = \frac{\pi}{2} - \arccos\sigma_1$ are angles between E^u and $E^n \oplus E^s$. The smallest singular values σ_2 of 2×2 matrices $\hat{\mathbf{P}}(t)$ are related to angles $\beta_2 = \frac{\pi}{2} - \arccos\sigma_2$ between $E^u \oplus E^n$ and E^s: both $\mathbf{u}_1$ and $\mathbf{u}_2$ span the 2-dimensional subspace $E^u \oplus E^n$, $\mathbf{v}_1$ and $\mathbf{v}_2$ are orthogonal to E^s.

We obtain statistics of angles β_1 and β_2 for sufficiently long trajectories. If there are zero angles, we conclude that the attractor is not hyperbolic. If distributions of angles β_1 and β_2 are both distanced from zero, then all subspaces are transversal and the attractor of the flow is uniformly hyperbolic according to our numerical approach. This also means that the attractor of the Poincaré cross-section is uniformly hyperbolic too.

It should be noted that the absence of zero angles β_k in numerical simulations is not a rigorous proof of hyperbolicity. Nonetheless, this technique allows us to distinguish between hyperbolic attractors and quasi-attractors easily and relatively quickly. Rigorous proofs must be based on checking the cone criteria[27,37,38].

Figure 5(a) displays the distributions of angles between subspaces of the flow attractor of system (4) at $\mu = 0.98$, $\alpha = 0.7$, $\varepsilon = 0.1$. The blue plot represents the distribution of angles β_1 between the unstable subspace E^u and its adjacent subspace $E^n \oplus E^s$, while the red plot represents the distribution of angles β_2 between the subspace $E^u \oplus E^n$ and the stable subspace E^s. Both distributions are distanced from zero, and an insert is included with a scaled part of the plots near minimal values. The minimal values of angles are $\beta_1^{min} = 0.0367$ and $\beta_2^{min} = 0.0066$, and zero angles are absent.

To cover all parts of the attractor, we checked 80 trajectories of duration $T_{dur} = 10000$ time units, with a timestep of the Runge – Kutta algorithm set to $\Delta t = 0.001$. Therefore, we conclude that the attractor of the flow system (4) is uniformly hyperbolic. For the sake of completeness, we also calculated the distribution between E^u and E^s subspaces of the attractor of the Poincaré return map, as shown in Fig. 5(b). The minimal value of the angle is $\beta_1^{min} = 0.1289$ for the Poincaré map. We checked 160 trajectories of duration $N_{dur} = 10^5$ points to cover all parts of the attractor.

Figure 6 shows a chart of regimes of the flow system (4), ε vs. μ at fixed value of $\alpha = 0.7$. The red region represents the domain of uniformly hyperbolic attractors of Smale – Williams type. This domain is continuous due to the structural stability of hyperbolic attractors. We checked numerous conditions simultaneously: (i) the largest Lyapunov exponent of the flow attractor is positive, (ii) the angles between subspaces of the flow attractor are never close to zero (we used a threshold of $\beta_{1,2}^{min} > 0.001$), and (iii) the expansion factor for the arguments of complex variables of the Poincaré map is 3, and the expansion is monotonous. The last condition narrows down the domain of hyperbolicity, but it is necessary to remove possible non-accurate results of the angle test (the lengths of the checked trajectories are finite, and possible zero angles may be missed). We found that attractors of Smale –

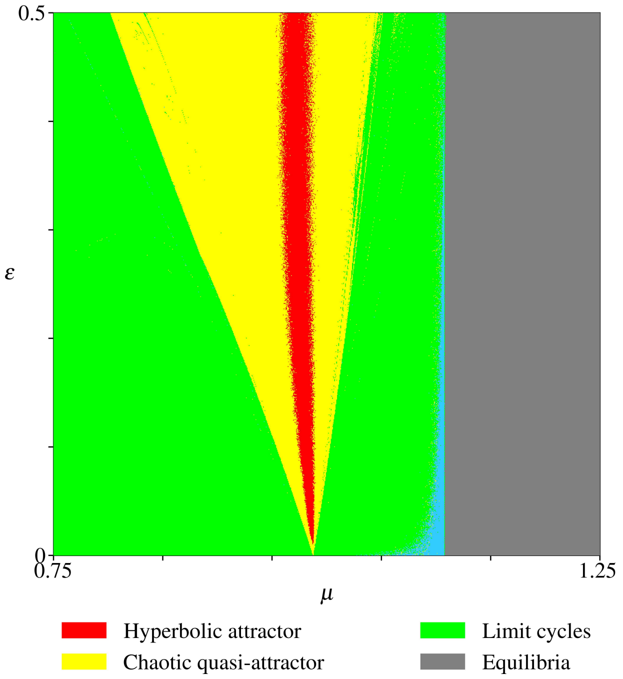

FIG. 6. The chart of regimes of the complex Shimizu – Morioka model (4), ε vs. μ, obtained numerically by calculating Lyapunov exponents, checking the transversality of tangent subspaces, and checking the expansion factor of the attractor. Here, $\alpha = 0.7$.

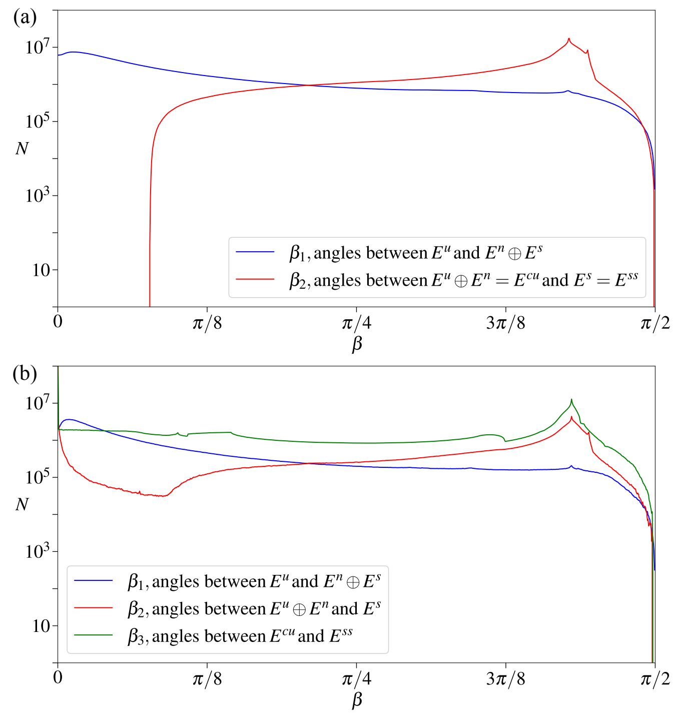

FIG. 7. (a) Distributions of angles between subspaces of the attractor of the classical Shimizu – Morioka system (2) at $\mu = 0.9$, $\alpha = 0.4$. (b) Distributions of angles between subspaces of the attractor of the modified complex Shimizu – Morioka system (4) at $\mu = 0.9$, $\alpha = 0.4$, with $\varepsilon = 0.1$.

Williams type are the only hyperbolic attractors.

The yellow region represents the domain of chaotic quasi-attractors, where the angle criteria is violated or the expansion of the argument is non-monotonous. The green region represents the domain of periodic cycles, where the largest Lyapunov exponent is zero. Finally, the grey region represents the domain of stable equilibria, where the largest Lyapunov exponent is negative.

The classical Shimizu – Morioka system (2) has a pseudo-hyperbolic Lorenz attractor at $\mu = 0.9$ and $\alpha = 0.4$. Pseudo-hyperbolic attractors satisfy the following conditions:

(i) the largest Lyapunov exponent is positive for every trajectory of the attractor,

(ii) the tangent space splits into strongly stable subspace E^{ss}, that contains only strongly contracting directions, and centrally unstable subspace E^{cu}, that expands volumes, but may include weakly contracting and neutral directions; the dimensions of E^{ss} and E^{cu} are the same for every trajectory,

(iii) subspaces E^{ss} and E^{cu} are transversal at every point of the attractor.

The classical Shimizu – Morioka attractor at $\mu = 0.9$, $\alpha = 0.4$ satisfies all of these conditions: (i) the largest Lyapunov exponent is $\lambda_1 = 0.0419 \pm 0.0005 > 0$, (ii) the sum $\lambda_1 + \lambda_2 = 0.0419 > 0$ ($\lambda_2 = 0$), therefore E^{cu} is 2-dimensional and includes expanding direction and neutral direction, $\lambda_3 = -1.3418 \pm 0.0004 < 0$, so E^{ss} is 1-dimensional. Lyapunov exponents of the saddle equilibrium also satisfy these conditions: $\lambda_1 = \frac{-\mu+\sqrt{\mu^2+4}}{2} = 0.646586$, $\lambda_2 = -\alpha = -0.4$, $\lambda_3 = \frac{-\mu-\sqrt{\mu^2+4}}{2} = -1.546586$, with a saddle value of $\sigma = \lambda_1 + \lambda_2 = 0.246586 > 0$, (iii) subspaces E^{ss} and E^{cu} are transversal (Fig. 7(a)). This method was used to reveal the domain of pseudohyperbolic Lorenz attractors on the chart from Fig. 2.

The Lorenz-like attractor at $\mu = 0.9$, $\alpha = 0.4$, $\varepsilon = 0.1$ is an interesting case (see Fig. 4(c-d)). The strongly stable subspace E^{ss} is 2-dimensional, and the centrally unstable subspace is 3-dimensional according to the Lyapunov exponents (6): $\lambda_1 + \lambda_2 + \lambda_3 = 0.0208 > 0$. The same is true for the saddle equilibrium, with Lyapunov exponents such that $\lambda_1 + \lambda_2 + \lambda_3 = -\mu + \sqrt{\mu^2+4} - \alpha = 0.893171 > 0$ and $\lambda_{4,5} = -1.546586 < 0$. Fig. 7(b) shows distributions of angles $\beta_{1,2,3}$, and importantly, the angles β_3 are zero at some points on the attractor, so the transversality of subspaces E^{cu} and E^{ss} is violated. Therefore, the flow attractor at $\mu = 0.9$, $\alpha = 0.4$, $\varepsilon = 0.1$ is not pseudohyperbolic. In fact, the Lyapunov exponents calculated in backward time with adjoint equations do not converge well in this case. One possible explanation is that there are trajectories embedded into the body of the attractor that are undetectable in forward time simulations and violate the pseudohyperbolicity condition (ii). However, the search for such trajectories is outside the scope of this work.

Fig. 8 shows a chart of regimes of the flow system (4), μ vs. α at fixed value of $\varepsilon = 0.1$. The red region represents the domain of uniformly hyperbolic attractors of Smale – Williams

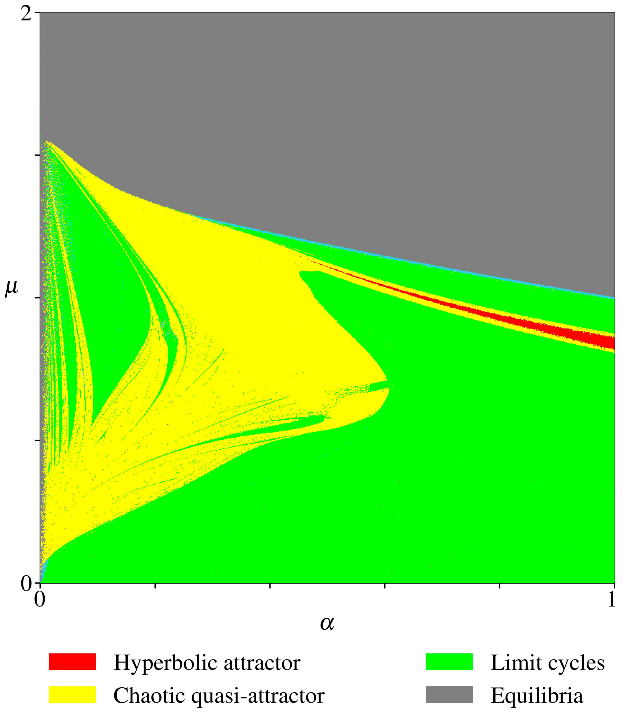

FIG. 8. The chart of regimes of the complex Shimizu – Morioka model (4), μ vs. α, obtained numerically by calculating Lyapunov exponents, by checking the transversality of tangent subspaces and by checking the expansion factor of the attractor. $\varepsilon = 0.1$. One can compare the chart with Fig. 2.

type. It is located near the line of homoclinic bifurcation with the negative saddle value in the original Shimizu – Morioka system (2), as can be seen by comparing with Fig. 2. The possibility of pseudohyperbolic attractors has also been checked, but none have been found in the complex system (4).

V. CONCLUSION

In this article, we introduced the modified complex Shimizu – Morioka system with a uniformly hyperbolic attractor of Smale – Williams type. Its operation is based on the "scattering" of trajectories on the saddle equilibrium in complex-valued systems that we have investigated before[3]. This new example is physically significant, with the only additional term not proposed before being εy^3. We added this term not because of its physical relevance, but to induce the instability of the angular variable, which is important to construct an attractor of Smale – Williams type. We surmise that any arbitrarily small holomorphic perturbation $h(y)$ to the second equation of the Shimizu – Morioka system can give rise to an attractor of Smale – Williams type, although this requires additional investigations.

We suppose that the mathematical phenomenon investigated in this article is quite general. We are aware of other examples with the same mechanism behind the formation of the attractor of Smale – Williams type[8,9,11].

The results presented in this article are numerical, and the construction and explanations are phenomenological. However, we are developing our approach to construct simple piece-wise models, where different parts of the phase space with different dynamics are glued together. This future development is in the spirit of works[54,55], where the Lorenz attractor is constructed by gluing linear systems of equations that govern different parts of the phase space.

ACKNOWLEDGMENTS

The work was carried out with the financial support of the Russian Science Foundation, Grant No. 21-12-00121 (https://www.rscf.ru/project/21-12-00121/). The authors thank Prof. Pavel Kuptsov, Prof. Dmitry Turaev and Prof. Vyacheslav Grines for useful discussions.

AUTHOR DECLARATIONS

The authors have no conflicts to disclose.

DATA AVAILABILITY

The data that support the findings of this study (computer programs, pictures) are available from the authors upon reasonable request.

[1] V. S. Afraimovich, V. Bykov, and L. P. Shilnikov, "On the origin and structure of the Lorenz attractor," in *Akademiia Nauk SSSR Doklady*, Vol. 234 (1977) pp. 336–339.
[2] V. Afraimovich, V. Bykov, and L. Shil'nikov, "On attracting structurally unstable limit sets of Lorenz type attractors," Trans. Moscow Math. Soc **44**, 153–216 (1983).
[3] S. Kuznetsov, V. Kruglov, and I. Sataev, "Smale – Williams solenoids in autonomous system with saddle equilibrium," Chaos: An Interdisciplinary Journal of Nonlinear Science **31**, 013140 (2021).
[4] D. Lyubimov and M. Zaks, "Two mechanisms of the transition to chaos in finite-dimensional models of convection," Physica D: Nonlinear Phenomena **9**, 52–64 (1983).
[5] A. Rovella, "The dynamics of perturbations of the contracting Lorenz attractor," Boletim da Sociedade Brasileira de Matemática-Bulletin/Brazilian Mathematical Society **24**, 233–259 (1993).
[6] A. Kazakov, "On bifurcations of Lorenz attractors in the Lyubimov – Zaks model," Chaos: An Interdisciplinary Journal of Nonlinear Science **31**, 093118 (2021).
[7] S. P. Kuznetsov, "Example of a physical system with a hyperbolic attractor of the Smale – Williams type," Physical review letters **95**, 144101 (2005).
[8] S. P. Kuznetsov and A. Pikovsky, "Autonomous coupled oscillators with hyperbolic strange attractors," Physica D: Nonlinear Phenomena **232**, 87–102 (2007).
[9] V. P. Kruglov, S. P. Kuznetsov, and A. Pikovsky, "Attractor of Smale – Williams type in an autonomous distributed system," Regular and Chaotic Dynamics **19**, 483–494 (2014).
[10] S. Kuznetsov, V. Kruglov, and Y. Sedova, "Mechanical systems with hyperbolic chaotic attractors based on Froude pendulums," Russian Journal of Nonlinear Dynamics **16**, 51–58 (2020).
[11] S. P. Kuznetsov, *Hyperbolic Chaos: A Physicist's View* (Higher Education Press: Beijing and Springer, 2012).
[12] A. Vladimirov, V. Y. Toronov, and V. Derbov, "Properties of the phase space and bifurcations in the complex Lorenz model," Technical Physics **43**, 877–884 (1998).
[13] A. Vladimirov, V. Y. Toronov, and V. L. Derbov, "The complex Lorenz model: Geometric structure, homoclinic bifurcation and one-dimensional map," International Journal of Bifurcation and Chaos **8**, 723–729 (1998).

[14] C.-z. Ning and H. Haken, "Detuned lasers and the complex Lorenz equations: subcritical and supercritical Hopf bifurcations," Physical Review A **41**, 3826 (1990).
[15] J. Gibbon and M. McGuinness, "The real and complex Lorenz equations in rotating fluids and lasers," Physica D: Nonlinear Phenomena **5**, 108–122 (1982).
[16] A. Fowler, J. Gibbon, and M. McGuinness, "The complex Lorenz equations," Physica D: Nonlinear Phenomena **4**, 139–163 (1982).
[17] J. Gibbon and M. McGuinness, "A derivation of the Lorenz equations for some unstable dispersive physical systems," Physics Letters A **77**, 295–299 (1980).
[18] A. Fowler, J. Gibbon, and M. McGuinness, "The real and complex Lorenz equations and their relevance to physical systems," Physica D Nonlinear Phenomena **7**, 126–134 (1983).
[19] E. N. Lorenz, "Deterministic nonperiodic flow," Journal of the atmospheric sciences **20**, 130–141 (1963).
[20] T. Shimizu and N. Morioka, "On the bifurcation of a symmetric limit cycle to an asymmetric one in a simple model," Physics Letters A **76**, 201–204 (1980).
[21] A. L. Shil'nikov, "On bifurcations of the Lorenz attractor in the Shimizu – Morioka model," Physica D: Nonlinear Phenomena **62**, 338–346 (1993).
[22] A. Shil'Nikov, L. Shil'Nikov, and D. Turaev, "Normal forms and Lorenz attractors," International Journal of Bifurcation and Chaos **3**, 1123–1139 (1993).
[23] D. V. Anosov, "Dynamical systems in the 1960s: the hyperbolic revolution," in *Mathematical events of the twentieth century* (Springer, 2006) pp. 1–17.
[24] S. Smale, "Differentiable dynamical systems," Bulletin of the American mathematical Society **73**, 747–817 (1967).
[25] D. Anosov, G. Gould, S. Aranson, V. Grines, R. Plykin, A. Safonov, E. Sataev, S. Shlyachkov, V. Solodov, A. Starkov, *et al.*, *Dynamical systems IX: dynamical systems with hyperbolic behaviour* (Springer, 1995).
[26] A. Katok and B. Hasselblatt, *Introduction to the modern theory of dynamical systems*, Vol. 54 (Cambridge university press, 1997).
[27] L. P. Shilnikov, "Mathematical problems of nonlinear dynamics: A Tutorial," International Journal of Bifurcation and Chaos **7**, 1953–2001 (1997).
[28] S. P. Kuznetsov, "Dynamical chaos and uniformly hyperbolic attractors: from mathematics to physics," Physics-Uspekhi **54**, 119 (2011).
[29] D. V. Turaev and L. P. Shil'nikov, "An example of a wild strange attractor," Sbornik: Mathematics **189**, 291 (1998).
[30] A. S. Gonchenko, S. V. Gonchenko, A. O. Kazakov, and A. Kozlov, "Elements of contemporary theory of dynamical chaos: a tutorial. part i. pseudohyperbolic attractors," International Journal of Bifurcation and Chaos **28**, 1830036 (2018).
[31] D. Turaev and L. Shil'nikov, "Pseudohyperbolicity and the problem on periodic perturbations of Lorenz-type attractors," in *Doklady Mathematics*, Vol. 77 (SP MAIK Nauka/Interperiodica, 2008) pp. 17–21.
[32] M. Malkin, "Topological conjugacy of discontinuous maps of a closed interval," Ukrainian Mathematical Journal **32**, 398–403 (1980).
[33] M. Malkin, "Rotation intervals and dynamics of Lorenz-like maps," Methods of Qualitative Theory of Differntial Equations , 122–139 (1985).
[34] S. Gonchenko, A. Kazakov, and D. Turaev, "Wild pseudohyperbolic attractor in a four-dimensional Lorenz system," Nonlinearity **34**, 2018 (2021).
[35] V. S. Afraimovich and S. L. P, "Strange attractors and quasi-attractors," in *Nonlinear Dynamics and Turbulence, eds. Barenblatt, G. I., Iooss, G. and Joseph, D. D.* (Pitman, New York, 1983) pp. 1–28.
[36] R. F. Williams, "Expanding attractors," Publications Mathématiques de l'Institut des Hautes Études Scientifiques **43**, 169–203 (1974).
[37] S. P. Kuznetsov and I. R. Sataev, "Hyperbolic attractor in a system of coupled non-autonomous van der Pol oscillators: Numerical test for expanding and contracting cones," Physics Letters A **365**, 97–104 (2007).
[38] D. Wilczak, "Uniformly hyperbolic attractor of the Smale – Williams type for a Poincaré map in the Kuznetsov system," SIAM Journal on Applied Dynamical Systems **9**, 1263–1283 (2010).
[39] L. P. Shilnikov, "On the generation of a periodic motion from trajectories doubly asymptotic to an equilibrium state of saddle type," Matematicheskii Sbornik **119**, 461–472 (1968).
[40] L. O. Chua, L. P. Shilnikov, A. L. Shilnikov, and D. V. Turaev, *Methods Of Qualitative Theory In Nonlinear Dynamics (Part II)*, Vol. 5 (World Scientific, 2001).
[41] G. Tigan and D. Turaev, "Analytical search for homoclinic bifurcations in the Shimizu – Morioka model," Physica D: Nonlinear Phenomena **240**, 985–989 (2011).
[42] M. J. Capiński, D. Turaev, and P. Zgliczyński, "Computer assisted proof of the existence of the Lorenz attractor in the Shimizu – Morioka system," Nonlinearity **31**, 5410 (2018).
[43] R. Barrio, A. Shilnikov, and L. Shilnikov, "Kneadings, symbolic dynamics and painting Lorenz chaos," International Journal of Bifurcation and Chaos **22**, 1230016 (2012).
[44] T. Xing, R. Barrio, and A. Shilnikov, "Symbolic quest into homoclinic chaos," International Journal of Bifurcation and Chaos **24**, 1440004 (2014).
[45] G. Benettin, L. Galgani, A. Giorgilli, and J.-M. Strelcyn, "Lyapunov characteristic exponents for smooth dynamical systems and for Hamiltonian systems; a method for computing all of them. Part 1: Theory," Meccanica **15**, 9–20 (1980).
[46] I. Shimada and T. Nagashima, "A numerical approach to ergodic problem of dissipative dynamical systems," Progress of theoretical physics **61**, 1605–1616 (1979).
[47] A. Pikovsky and A. Politi, *Lyapunov exponents: a tool to explore complex dynamics* (Cambridge University Press, 2016).
[48] P. V. Kuptsov, "Fast numerical test of hyperbolic chaos," Physical Review E **85**, 015203 (2012).
[49] P. V. Kuptsov and S. P. Kuznetsov, "Lyapunov analysis of strange pseudohyperbolic attractors: angles between tangent subspaces, local volume expansion and contraction," Regular and Chaotic Dynamics **23**, 908–932 (2018).
[50] P. Frederickson, J. L. Kaplan, E. D. Yorke, and J. A. Yorke, "The Liapunov dimension of strange attractors," Journal of differential equations **49**, 185–207 (1983).
[51] Y.-C. Lai, C. Grebogi, J. Yorke, and I. Kan, "How often are chaotic saddles nonhyperbolic?" Nonlinearity **6**, 779 (1993).
[52] V. S. Anishchenko, A. Kopeikin, J. Kurths, T. Vadivasova, and G. Strelkova, "Studying hyperbolicity in chaotic systems," Physics Letters A **270**, 301–307 (2000).
[53] P. V. Kuptsov and U. Parlitz, "Theory and computation of covariant Lyapunov vectors," Journal of nonlinear science **22**, 727–762 (2012).
[54] V. N. Belykh, N. V. Barabash, and I. V. Belykh, "A Lorenz-type attractor in a piecewise-smooth system: Rigorous results," Chaos: An Interdisciplinary Journal of Nonlinear Science **29**, 103108 (2019).
[55] V. N. Belykh, N. V. Barabash, and I. V. Belykh, "Sliding homoclinic bifurcations in a Lorenz-type system: Analytic proofs," Chaos: An Interdisciplinary Journal of Nonlinear Science **31**, 043117 (2021).